EBG Common-Mode Filter Design Using Uncoupled Coplanar Waveguide to Microstrip Transitions

Wilder A. Alarcon, A. Ege Engin, *Member, IEEE,*
Ivan Ndip, *Senior Member, IEEE,* and Klaus-Dieter Lang, *Senior Member, IEEE*

***Abstract*—This letter investigates the effects of an Electromagnetic Bandgap (EBG) common-mode filter design using coplanar waveguide (CPW) to microstrip transitions on differential signals. Specifically, the improvements in the frequency and time domains are studied by s-parameters and eye diagrams. EBG structures are based on a periodic alteration of even-mode impedances to create stop bands in the common-mode, while not affecting the differential mode as much as possible. The proposed common-mode filter is unique in the way that a broad bandwidth is achieved by choosing one of the even-mode characteristic impedances as small as possible. This EBG structure is implemented on a printed circuit board (PCB) and characterized using a 4-port vector network analyzer (VNA).**

***Index Terms*—Electromagnetic band-gap (EBG), mixed-mode S-parameters, even and odd mode impedances, common-mode filters, eye diagram simulations, signal integrity (SI).**

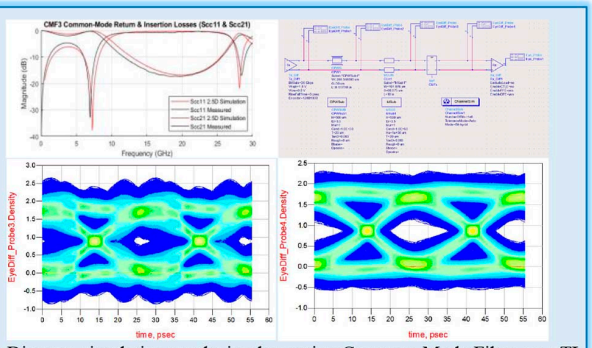

Eye Diagram simulation results implementing Common-Mode Filter on a TL with 90° skew at the driver. (Top Left: Common-Mode Filter Mixed -Mode S-Parameters. Top Right: simulation setup. Bottom Left: Eye diagram before common-mode filter. Bottom Right: Eye diagram results after common-mode filter.)

I. Introduction

As TECHNOLOGY advances, there is a need to move data between integrated circuits (ICs) at high data rates/frequencies. As the speed increases, some second-order noise issues that were neglected at lower frequencies become more significant and increase the complexity of the design [1]. It has been shown that differential traces can obtain up to twice the bit rate for the same net length than a single ended trace [2]. Along with being able to transmit and receive at higher speeds, using differential traces can help reduced effects of external noise, such as crosstalk, power supply noise, or electromagnetic interference (EMI).

Differential signaling can however suffer from unwanted common-mode noise which most of the time gets ignored at lower speeds. This common-mode noise gets introduced into a system by skews in trace lengths, driver timing discrepancies, and substrate inhomogeneity due to glass-weave effect. These lead to signal integrity issues.

Manuscript received April 15, 2020; revised June 25, 2020; accepted August 17, 2020. Date of publication August 25, 2020; date of current version December 18, 2020. This work was supported by Alexander von Humboldt Foundation. *(Corresponding author: Wilder A. Alarcon.)*

Wilder A. Alarcon and A. Ege Engin are with the Electrical Engineering Department, San Diego State University, San Diego, CA 92182 USA (e-mail: walarcon@sdsu.edu; aengin@sdsu.edu).

Ivan Ndip and Klaus-Dieter Lang are with the Fraunhofer-Institut fuer Zuverlaes-sigkeit und Mikrointegration IZM, 82234 Berlin, Germany (e-mail: ivan.ndip@izm.fraunhofer.de; klaus-dieter.lang@izm.fraunhofer.de).

Digital Object Identifier 10.1109/LEMCPA.2020.3019449

In previous studies [3], it has been shown that common-mode amplitudes can be in the same order as differential-mode amplitudes and can degrade the eye-diagram at the receiver. The effects of common-mode amplitudes can cause bit errors and potentially cause a system to fail. Common-mode noise filters for EMI suppression have been introduced before using common-mode chokes [4], [5], which however are effective at frequencies under 1GHz as they have high insertion losses at high frequencies and are not designed for a specific frequency band.

There are multiple approaches of using periodic EBG structures to try to filter out the common-mode noise in differential

Take-Home Messages:

- Differential traces can help transmit data at high speeds in the presence of crosstalk, power-supply noise, and electromagnetic interference.
- Common-mode noise introduced by P-N skews, driver timing discrepancies and impedance mismatches due to glass-weave effect still affect performance.
- EBG structures can be used to create common-mode filters to eliminate the common-mode noise without affecting the differential mode transmission.
- This type of common-mode filter can be used in very high-speed applications as the length of the filter is directly proportional to the center frequency of the filter (quarter-wavelength).

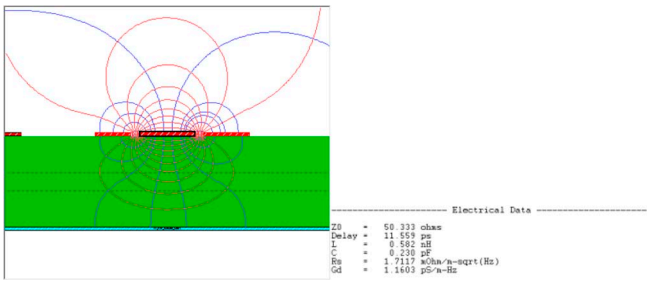

Fig. 1. Coplanar waveguide line with 50Ω even and odd-mode impedances.

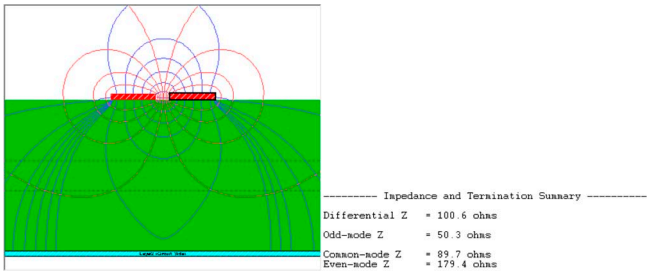

Fig. 2. Differential microstrip TL with 180Ω even-mode and 50Ω odd-mode impedances.

lines in the events of IC to IC communication or communication between printed circuit boards (PCBs) using connectors or cables. Many types of EBG structures can be implemented as common-mode filters such as the EBG structures on the reference planes or planar EBGs [6]–[9]. We have recently studied common-mode filters in differential lines as stepped-impedance filters [10]. In this letter, we will introduce a new effective common-mode filter using coplanar waveguide (CPW) and differential microstrip lines and summarize the effect of this filter in the frequency and time domains using s-parameters and eye diagram simulations.

II. EBG Structures

A. Even and Odd Mode Impedance

In [10], design equations to determine the on-set and off-set frequencies of the EBG common-mode stopband were derived. As a result, the fractional bandwidth of the filter can be calculated using

$$BW = 2 - \frac{4}{\pi}\cos^{-1}\left(\frac{Z_e^h - Z_e^l}{Z_e^h + Z_e^l}\right) \tag{1}$$

where Z_e^h and Z_e^l are the high and low even-mode characteristic impedances of the filter sections. Therefore, higher separation between even and odd mode impedances on a differential line results in broader bandwidth for the common-mode filter.

Even and odd-mode impedances can be calculated from the per unit length elements of the inductance and capacitance matrices as

$$Z_e = \sqrt{\frac{L_{11} + L_{12}}{C_{11} + C_{12}}} \tag{2}$$

$$Z_o = \sqrt{\frac{L_{11} - L_{12}}{C_{11} - C_{12}}} \tag{3}$$

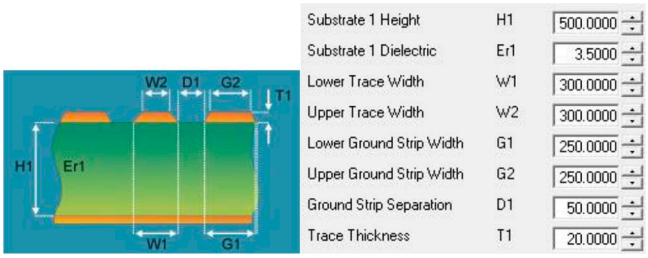

Fig. 3. CPW stackup & dimensions (in microns).

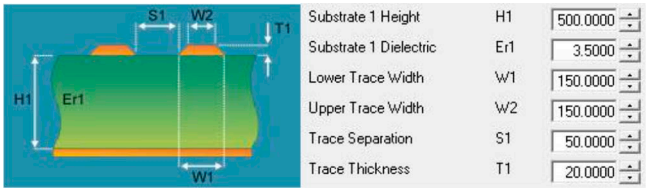

Fig. 4. Differential microstrip stackup & dimensions (in microns).

indicating that $Z_e \geq Z_o$, since the mutual capacitance C_{12} is always negative. In this letter we propose a unique design by choosing $Z_e^l = Z_o$, in order to achieve largest bandwidth.

As an example, we designed two different differential lines: one with 50Ω odd and even-mode impedances, and one with 50Ω odd-mode impedance and 180Ω even-mode impedance. The 50Ω odd and even-mode impedances were achieved using coplanar waveguides (CPW) as shown in Figure 1, while the 50Ω odd/180Ω even impedances were achieved using a tightly-coupled microstrip differential line as shown in Figure 2. The CPWs have negligible coupling due to the ground trace in between the two signal lines as shown in Figure 5, resulting in equal even and odd mode impedances.

By keeping the odd-mode impedance constant while periodically varying the even-mode impedance, we can create a stepped-impedance common-mode filter [11], [12].

B. PCB Design

Based on the extracted values from the 2D simulation, we designed the EBG structure on a printed circuit board with Rogers RO4003 and RO4450F for the cores and prepreg, respectively. For the CPW, we used a width of 300 microns with a spacing of 50 microns to co-planar reference as shown in Figure 3. For the differential microstrip, we used trace widths of 150 microns with a separation of 50 microns displayed in Figure 4. The copper thickness for all traces and ground plane is 20 microns. The filter is designed to have a CMF at a specific frequency by selecting its respective quarter wavelength as the length of each section. In this case, lengths of 2.6mm and 2.35mm for the CPW and differential microstrip, respectively, were used to have a center frequency of 18GHz, in order to effectively filter a 36Gbps signal.

Three different filters were analyzed. One with three CPW sections and two differential microstrip sections (CMF3), another with six CPW sections and five differential microstrip sections (CMF6), and lastly, one with eight CPW sections and seven differential microstrip sections (CMF8). An image of CMF3 implemented on the PCB can be seen in Figure 5.

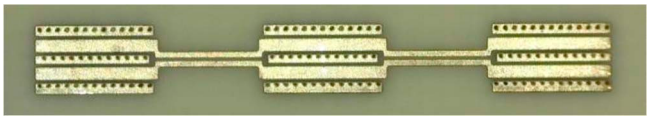

Fig. 5. Implementation of CMF3 on a PCB.

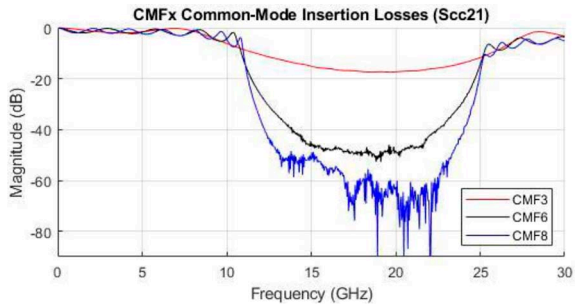

Fig. 6. Measured common-mode insertion loss ($S_{cc}21$) of 3 designs.

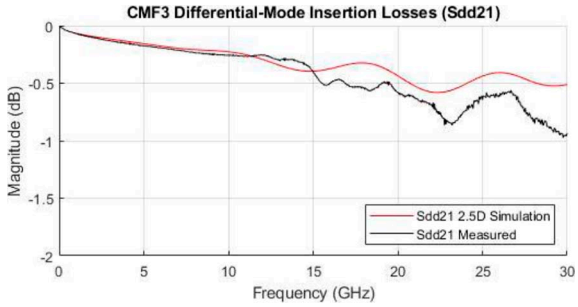

Fig. 7. S_{DD21} of CMF3.

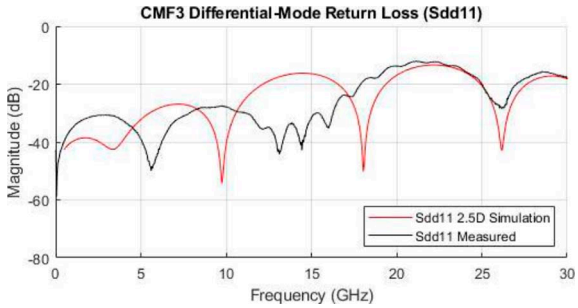

Fig. 8. S_{DD11} of CMF3.

III. Simulated vs Measured Mixed-Mode S-Parameters

Mixed-mode s-parameters were characterized using 250um GSGSG micro probes on a E8361A 4-port VNA with a Short-Open-Load-Through (SOLT) calibration to verify the EBG structures' effects on the differential and common modes. The objective is to create a common-mode bandstop filter at a certain frequency range without affecting the differential-mode. Figure 6 displays the extracted common-mode insertion loss from all three designs. With increasing number of unit cells, the isolation level of the CMF increases as expected.

The CMFs were also simulated with a 2.5D simulator that considers the transitions between the CPW and differential microstrip sections. Figures 7 through 9 display the differential-mode insertion and return loss (S_{DD21}&S_{DD11}) and

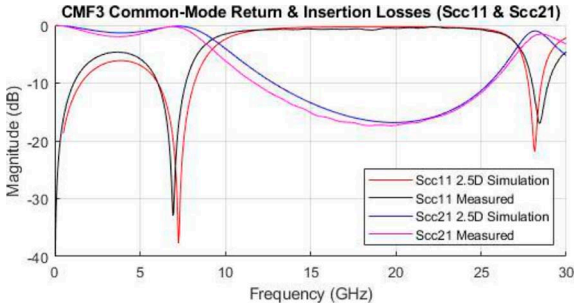

Fig. 9. S_{CC11}&S_{CC21} of CMF3.

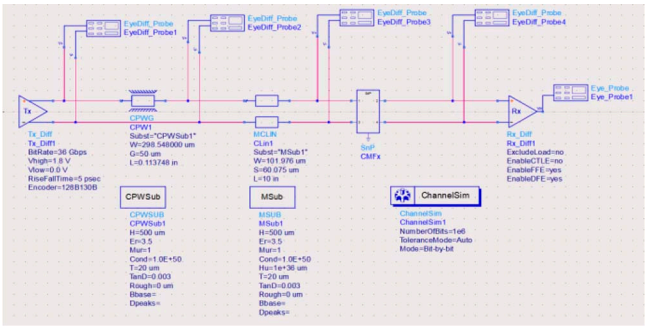

Fig. 10. Eye diagram schematic using 90° skew at the driver, 100Ω differential TL and CMF3 S-Parameter model.

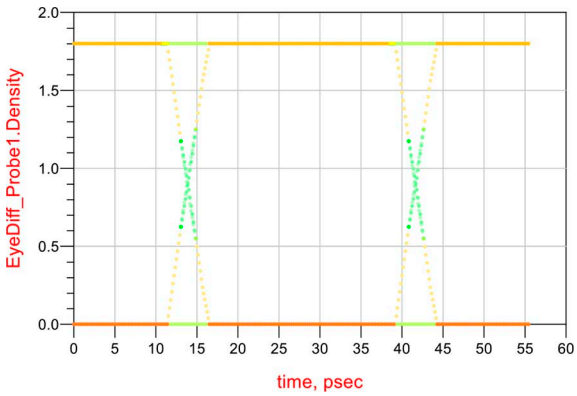

Fig. 11. Eye diagram after differential driver.

common-mode insertion and return loss (S_{CC21}&S_{CC11}) of CMF3. Figures 7 and 8 indicate that the differential mode is not significantly affected by the insertion of the CMF. The simulated and measured values show good correlation in Figures 7, 8 and 9.

Based on these results, this EBG structured common-mode filter provides a band-stop filter centered at 18GHz, without having significant effect on the differential mode.

IV. Eye Diagram Simulations

Figure 10 shows the eye diagram simulation setup, implementing a 90° skew on the positive leg of the driver in the form of a 50Ω CPW (similar to the coplanar section in the EBG common-mode filter); a differential microstrip line (similar to the one we are using in our common mode filter) with a differential impedance of 100Ω; and the CMF3 filter. The addition of the 90° skew is implemented to cause the horizontal part of

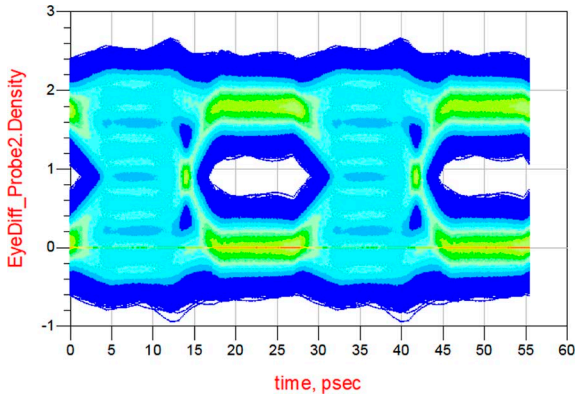

Fig. 12. Eye diagram after 90° skew.

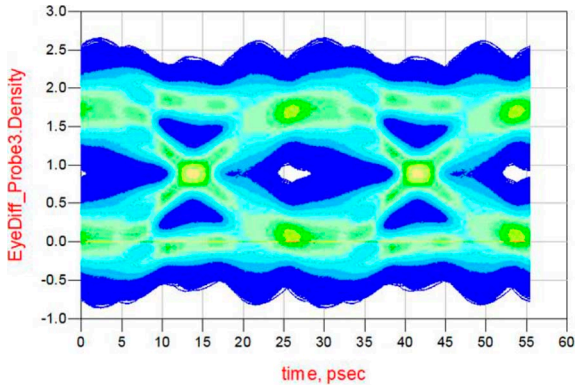

Fig. 13. Eye diagram after 90° skew and 100Ω differential TL.

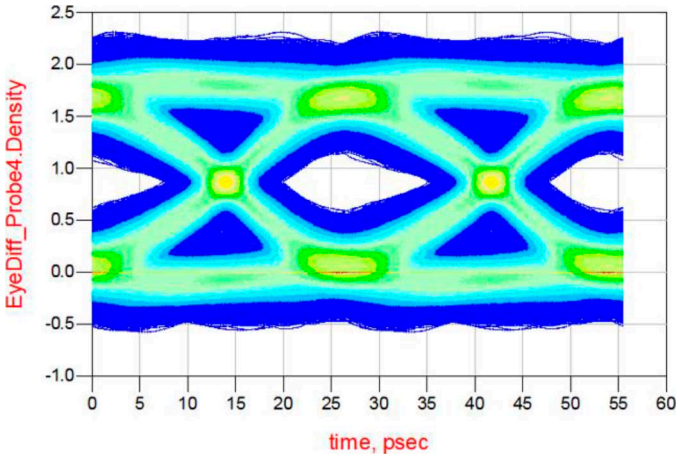

Fig. 14. Eye diagram after 90° skew, 100Ω differential TL, and CMF3 S-Parameter model.

the eye to close by half as seen on figures 11 and 12. Four different differential eye probes were added, one after the driver, one after the 90° skew, one after the differential TL, and one after the CMF3 common-mode filter s-parameter model.

Figures 11-14 display the eye diagram immediately following the driver, 90° skew, the differential microstrip line, and after the CMF3 filter, respectively. CMF6 and CMF8 were also simulated with similar results. It can be observed that the eye diagram is almost completely closed after the 90° skew and the differential line in Figure 13. The CMF helps to mitigate these effects by reopening the eye as shown in Figure 14.

V. Conclusion

A new EBG common mode filter is proposed which is unique in the way that the smallest possible even-mode characteristic impedance is used. The effectiveness in the frequency and time domains are verified using measured mixed-mode S-parameters and simulated eye diagrams. In the frequency domain, a stopband in the common mode is observed in agreement with the design equations without significantly affecting the differential mode. In the time domain, we can see the filter improves the eye and therefore improving the distortion and jitter. As data speeds increase, this filter can be used to mitigate common-mode noise in differential signals. The higher the frequency, the shorter the filter's length and therefore this common-mode filter can be very useful in very high-speed applications.

Acknowledgment

The authors would like to thank Gabriel Wieland from Fraunhofer IZM for the RF characterization of the common-mode filters.

References

[1] M. S. Sharawi, "Practical issues in high speed PCB design," *IEEE Potentials*, vol. 23, no. 2, pp. 24–27, Apr./May 2004.

[2] Z. Chen and G. Katopis, "A comparison of performance potentials of single ended vs. differential signaling," in *Proc. Elect. Perform. Electron. Packag.*, Portland, OR, USA, 2004, pp. 185–188.

[3] S. Connor, B. Archambeault, M. Mondal, "The impact of common mode currents on signal integrity and EMI in high-speed differential data links," in *Proc. IEEE Int. Symp. Electromagn. Compat.*, Detroit, MI, USA, 2008, pp. 1–5.

[4] M. Damnjanovic, L. Zivanov, and G. Stojanovic, "Common mode chokes for EMI suppression in telecommunication systems," in *Proc. IEEE Int. Conf. Comput. Tool EUROCON*, Warsaw, Poland, 2007, pp. 905–909.

[5] N. Oka, K. Misu, S. Yoneda, S. Saito, and S. Nitta, "A common mode noise filter for high speed and wide band differential mode signal transmission," in *Proc. 10th Int. Symp. Electromagn. Compat.* York, U.K., 2011, pp. 732–736.

[6] F. de Paulis, L. Raimondo, S. Connor, B. Archambeault, and A. Orlandi, "Design of a common mode filter by using planar electromagnetic bandgap structures," *IEEE Trans. Adv. Packag.*, vol. 33, no. 4, pp. 994–1002, Nov. 2010.

[7] M. Pajovic, J. Savic, A. Bhobe, and X. Zhou, "The gigahertz two-band common-mode filter for 10-Gbit/s differential signal lines," in *Proc. IEEE Int. Symp. Electromagn. Compat.*, Denver, CO, USA, 2013, pp. 472–477.

[8] N. P. Modi, A. Olivera, A. E. Engin, and H. Oomori, "Resonant-plane common-mode filter in differential lines," in *Proc. IEEE CPMT Symp. Jpn. (ICSJ)*, Kyoto, Japan, 2017, pp. 235–238.

[9] A. E. Engin, N. Modi, and H. Oomori, "Stepped-impedance common-mode filter for differential lines enhanced with resonant planes," *IEEE Trans. Electromagn. Compat.*, vol. 61, no. 5, pp. 1457–1464, Oct. 2019.

[10] A. E. Engin, "Stepped-impedance common-mode filter in differential lines," in *Proc. IEEE CPMT Symp. Jpn. (ICSJ)*, Kyoto, Japan, 2016, pp. 209–212.

[11] S. Oh, J. Jeong, and J. Lee, "Wideband common noise suppression filter based on coupled microstrip lines and edge-coupled coplanar waveguides," *Electron. Lett.*, vol. 51, no. 25, pp. 2123–2124, Dec. 2015.

[12] M. Cracraft and S. Connor, "Mode-selective periodic transmission line filters to reduce radiated common-mode emissions," in *Proc. IEEE Int. Symp. Electromagn. Compat.*, Ottawa, ON, Canada, Jul. 2016, pp. 216–221.